1994-09

Modelling tools for active classification in shallow water environments

Huelsnitz, Warren G.

Monterey, California. Naval Postgraduate School

NAVAL POSTGRADUATE SCHOOL
Monterey, California

THESIS

MODELLING TOOLS FOR
ACTIVE CLASSIFICATION IN
SHALLOW WATER ENVIRONMENTS

by

Warren G. Huelsnitz

September, 1994

Thesis Advisors: James H. Miller
Ching-Sang Chiu

REPORT DOCUMENTATION PAGE

Form Approved OMB No. 0704-0188

1. AGENCY USE ONLY *(Leave blank)*	2. REPORT DATE September, 1994	3. REPORT TYPE AND DATES COVERED Master's Thesis

4. TITLE AND SUBTITLE MODELLING TOOLS FOR ACTIVE CLASSIFICATION IN SHALLOW WATER ENVIRONMENTS

5. FUNDING NUMBERS

6. AUTHOR(S) Warren G. Huelsnitz

7. PERFORMING ORGANIZATION NAME(S) AND ADDRESS(ES)
Naval Postgraduate School
Monterey CA 93943-5000

8. PERFORMING ORGANIZATION REPORT NUMBER

9. SPONSORING/MONITORING AGENCY NAME(S) AND ADDRESS(ES)

10. SPONSORING/MONITORING AGENCY REPORT NUMBER

11. SUPPLEMENTARY NOTES The views expressed in this thesis are those of the author and do not reflect the official policy or position of the Department of Defense or the U.S. Government.

12a. DISTRIBUTION/AVAILABILITY STATEMENT
Approved for public release; distribution is unlimited.

12b. DISTRIBUTION CODE
A

13. ABSTRACT *(maximum 200 words)*

Several tools have been developed, primarily using MATLAB, for modeling the active return of a target in an arbitrary, three-dimensional ocean environment and for quantifying the environmental distortion and interference. An acoustic model based on ray theory is used to compute the target echo and reverberation. These tools have been applied to Barents Sea and Gulf of Sidra ocean environments for a billboard transmit/receive array of 25 equally spaced elements.

The frequency dependence of a sonar target's echo depends on its size, shape, wall thickness, and acoustic impedance. Active classification involves using this 'signature', or transfer function, to classify the target and reduce or eliminate false alarms. Complications arise due to the signal distortion that occurs in inhomogeneous ocean environments, particularly in shallow water. Multiple paths, reverberation, and ambient noise modify the received signal and make it difficult to extract the target's response. It is hoped that these tools will provide insight into the modelling and signal processing requirements for active classification as well as realistic signals for testing various schemes.

14. SUBJECT TERMS active sonar, shallow water, classification, acoustic modelling			15. NUMBER OF PAGES 53
			16. PRICE CODE
17. SECURITY CLASSIFICATION OF REPORT Unclassified	18. SECURITY CLASSIFICATION OF THIS PAGE Unclassified	19. SECURITY CLASSIFICATION OF ABSTRACT Unclassified	20. LIMITATION OF ABSTRACT UL

NSN 7540-01-280-5500

Standard Form 298 (Rev. 2-89)
Prescribed by ANSI Std. 239-18

Approved for public release; distribution is unlimited.

Modelling Tools for
Active Classification in
Shallow Water Environments

by

Warren G. Huelsnitz
Lieutenant, United States Navy
B.S., University of Minnesota, 1987

Submitted in partial fulfillment
of the requirements for the degrees of

MASTER OF SCIENCE IN APPLIED PHYSICS
and
MASTER OF SCIENCE IN PHYSICAL OCEANOGRAPHY

from the
NAVAL POSTGRADUATE SCHOOL
September 1994

Author: [redacted]
Warren G. Huelsnitz

Approved by: [redacted]
James H. Miller, Thesis Advisor

[redacted]
Ching-Sang Chiu, Co-Advisor

[redacted]
Robert M. Keolian, Third Reader

[redacted]
William B. Colson, Chairman, Dept. of Physics

[redacted]
Robert H. Bourke, Chairman, Dept. of Oceanography

ABSTRACT

Several tools have been developed, primarily using MATLAB, for modeling the active return of a target in an arbitrary, three-dimensional ocean environment and for quantifying the environmental distortion and interference. An acoustic model based on ray theory is used to compute the target echo and reverberation. These tools have been applied to Barents Sea and Gulf of Sidra ocean environments for a billboard transmit/receive array of 25 equally spaced elements.

The frequency dependence of a sonar target's echo depends on its size, shape, wall thickness, and acoustic impedance. Active classification involves using this 'signature', or transfer function, to classify the target and reduce or eliminate false alarms. Complications arise due to the signal distortion that occurs in inhomogeneous ocean environments, particularly in shallow water. Multiple paths, reverberation, and ambient noise modify the received signal and make it difficult to extract the target's response. It is hoped that these tools will provide insight into the modelling and signal processing requirements for active classification as well as realistic signals for testing various schemes.

TABLE OF CONTENTS

LIST OF FIGURES

ACKNOWLEDGEMENTS

I would like to express my sincere gratitude and appreciation for the guidance, insight, and inspiration provided by my thesis advisors, Professor James H. Miller and Professor Ching-Sang Chiu. Throughout the many months that I have been working on this project, they have patiently and effectively steered my efforts along productive pathways and kept me from wandering too far astray. I would also like to thank Professor Robert M. Keolian who served as a reader from the Physics Department and provided a physicist's perspective.

I would like to thank Laura Ehret and John Mykyta for getting me up and running with HARPO, Le Ngoc Ly for assistance with the Mediterranean data files, Naval Research Laboratory for providing the target model, and the various oceanography and physics instructors I've had here at the Naval Postgraduate School who have instilled me with the necessary knowledge and curiosity to attempt such a project.

Lastly, I would like to thank my family for their patience and understanding during the many days and weeks they've had to put up with my absence due to long hours of thesis research and writing.

I. INTRODUCTION

The nature of warfare at sea has evolved dramatically in recent years due to changing political as well as technological climates around the world. As projected missions continue to send the Navy into shallow water and littoral regions, the submarine and mine threats pose significant problems. Shallow water is acoustically much more complicated than deep water, open ocean regions. Additionally, advances in submarine technology have made extremely quiet and capable platforms available to potential adversaries. Active systems, required for detection of such platforms, generate numerous false alarms. The ability to detect submarines or mines and eliminate false alarms would ensure battlespace dominance with fewer dedicated assets.

Active classification offers a method by which detections could be classified as either natural or manmade based on characteristics in the target's echo. In order to examine the potential usefulness of an active classification system or algorithm, it is necessary to consider the impact of the environment. Towards this goal, methods have been developed for modelling target echos and reverberation in arbitrary ocean environments. These tools can be used to model the performance of user-defined source and receiver arrays and the user's choice of transmitted signal and target model. The programs involved and some examples will be discussed along with some of the implications for active classification.

A. ACTIVE CLASSIFICATION

Active classification involves using the frequency and/or aspect dependence of a target's complex scattering function to recognize and hence classify the target. The scattered field is the superposition of various modes excited by the incident wave. These modes include specularly reflected components, geometrically transmitted components, circumferential surface waves, and creeping waves which diffract around the perimeter of the target. Nulls and peaks in the scattering function are determined by the size, shape, wall thickness, and acoustic impedance of the object. Classification of a target based on these features is similar to spectroscopic identification of chemical elements.

Several classification experiments have been performed on small targets, with appropriately scaled wavelengths, using theoretically and empirically derived scattering functions. See, for example, Chestnut et al., (1979) or Svardstrom (1993). Automated classification algorithms have been quite successful when the signal to noise ratio is large. But any noise in the received signal severely degrades classification performance. The noise added to experimental signals to simulate real world conditions is often white, gaussian noise. We will see that a realistic environment distorts and disrupts the received signal and adds a significant amount of noise, reverberation, and multi-path interference.

Complications arise because the oceanic transfer function depends on many factors and the received signal is affected by much more than one's choice of transmitted signal and the target's acoustic scattering characteristics. Surface and

bottom interactions, multiple paths, and absorption distort the signal. Ambient noise and reverberation can overwhelm the target's echo. Additionally, the sound speed field is a function of time as well as all three spatial dimensions. Source, receiver, and target motion also modify the received signal.

Various methods, (experimental, analytical, and numerical), exist for predicting a target's complex scattering function. But extracting classification features from signals contaminated with noise and reverberation and distorted by the ocean environment may require sophisticated signal processing techniques, such as neural networks or adaptive filters. Such techniques are beyond the scope of the present study. It is, however, hoped that the following will provide some insight into the signal processing requirements for active classification as well as realistic signals for testing various classification algorithms or systems.

B. OVERVIEW OF THESIS

The objective of this thesis has been to develop the tools necessary for modelling the active return of a target in an arbitrary, two or three dimensional, ocean environment. Acoustic modelling is accomplished using ray theory. The impact of surface and bottom interactions, multiple paths, boundary reverberation, and ambient noise have been included. Volume reverberation and absorption are small for the frequencies considered here and have been neglected but could readily be incorporated. Temporal variability and fluctuations of the sound speed field due to various phenomenon such as currents, internal waves, and turbulence are likely to have a

significant impact on active classification but have not been treated. The source/receiver platform is considered fixed but the target is allowed to move.

Chapter II will introduce the various building blocks and components of the modelling scheme. Then, the modelling of various physical phenomenon will be discussed in detail. Chapter III introduces the ocean environments, target model, and the source and receiver array used in the case study. The resulting signals for some specific cases and illumination of various environmental factors will then be discussed. Crosscorrelations between modelled signals and uncontaminated reference signals were used to evaluate the distortion induced by the oceanic channel. Finally, Chapter IV discusses the conclusions of the present study and Chapter V presents some recommendations for further efforts.

An operational classification scheme will probably use adaptive filters and neural networks. This work will hopefully provide insight into the modeling and processing requirements as well as realistic signals for testing classification algorithms and evaluating system performance. By creating realistic, synthetic signals in a 'virtual' ocean, we could predict system performance in a region where we are not able to physically test it as well as perhaps tailor the classification algorithm to the region.

II. COMPONENTS OF THE MODEL

Three-dimensional numerical raytracing was performed by the NOAA Hamiltonian Acoustic Raytracing Program for the Ocean (HARPO) (Jones et al., 1986). HARPO is a FORTRAN-based program that requires a three-dimensional sound speed field and a two-dimensional bathymetry field as input. The output of HARPO is then submitted to a program, written in MATLAB, called "rbreak.m". This program, originally written by Ching-Sang Chiu in 1993 and modified to aid in reverberation calculations, conducts eigenray searches and computes the cumulative effects of ray tube spreading and surface and bottom interactions for each ray.

Two additional MATLAB programs, "xfer.m" and "xferreverb.m", use the output of rbreak.m. The first incorporates a target model, a user defined source and receiver, and a transmitted signal and creates artificial target echos for a band of target range and depth points. The second uses generic reverberation formulas to compute boundary reverberation and to create a synthetic reverberation signal that overlaps the arrival of the target's echo. As will be discussed later, xfer.m can also provide false target echos, either by using a different target model or a frequency independent model already in place. These false echos can then be compared to valid targets.

An artificial ambient noise signal is created by "ambient.m". This program does not presently involve any environmental dependence beyond using an omnidirectional noise spectrum for the region of interest, which is then adjusted for

the directionality of the receiver. From this, a time series of ambient noise is created.

The details of the acoustic modelling for various components of a realistic signal will be discussed in the following sections. A received signal consists of ambient noise, reverberation, and possibly a target echo and/or the echos from various false targets.

A. MULTI-PATH EFFECTS

After HARPO has traced a set of ray paths for a specific source/receiver location, rbreak.m performs an eigenray search to find all rays striking a point-like target at various locations within the water column. Several acoustic parameters, including surface loss, bottom loss, travel time, ray tube spreading, and accumulated phase shifts due to boundary interactions and turning points are tabulated.

The affect of ray tube spreading is approximated using the formula (Clay and Medwin, 1977, p. 93):

$$\frac{P}{P_{1m}} = \sqrt{\frac{\Delta_\theta \, c \cos\theta_0}{r \, h \, c_0 \cos\theta}} \qquad (1)$$

where P_{1m}, c_0, and Θ_0 are the pressure, sound speed, and ray elevation angle one meter from the source and P, c, and Θ are the equivalent parameters at range r. Δ_θ is the increment between adjacent launch angles and h is the vertical separation between adjacent rays at range r.

Surface scattering is computed using the formula of Brekhovskikh and Lysanov, (1982, p. 180):

$$\frac{P_{scat}}{P_{inc}} = \exp(-2\, k^2\, \sigma^2\, \sin^2\theta) \tag{2}$$

where k is the wave number, θ is the ray elevation angle, and σ is the rms waveheight or bottom roughness. Each bottom interaction is computed using Equation (2) multiplied by the formula of Clay and Medwin, (1977, p. 63):

$$\frac{P_{scat}}{P_{inc}} = \frac{\rho_b\, c_b \cos\theta - \rho\, c \cos\theta_b}{\rho_b\, c_b \cos\theta + \rho\, c \cos\theta_b} \tag{3}$$

where the subscript b refers to the bottom and

$$\theta_b = \sin^{-1}\left(\frac{c}{c_b}\sin\theta\right) \tag{4}$$

In accordance with Brekhovskikh (1980, p. 204), a phaseshift of $-\pi/2$ is applied to each turning point. A phaseshift of $-\pi$ is assumed for each surface interaction and the phaseshift due to each bottom interaction is given by the complex result of Equation (3). Note that scattering and transmission occurs at the bottom but only scattering occurs at the surface.

The tabulated parameters for each eigenray are then combined with a synthetic signal and a target model using the MATLAB program xfer.m to create a simulated echo resulting from multipath effects. The received signal Y(f) is given by:

$$Y(f+\Delta f_i+\Delta f_j) = \sum_i \sum_j X(f)\, B_S(f,\theta_i,\phi_i) \cdot H_i(f,\theta_i,\phi_i)\, \sigma_t(f+\Delta f_i,\theta_i,\phi_i,\theta_j,\phi_j) \cdot H_j(f+\Delta f_i+\Delta f_j,\theta_j,\phi_j)\, B_R(f+\Delta f_i+\Delta f_j,\theta_j,\phi_j) \quad (5)$$

where

X = *Transmitted Signal*
$B_{S,R} = b(\theta_{i,j})\ b(\phi_{i,j})$ (*srce/rcvr beam patterns*)
$H_{i,j}$ = *oceanic transfer function for ray i,j*
$\Delta f_{i,j}$ *represents the doppler shift*

The indices i and j refer to ray paths from source to target and from target to receiver, respectively.

In the computations, acoustic rays are individually doppler-shifted, accounting for the angles at which they strike and leave the target and the target's speed. The angle at which a ray strikes the cylindrically symmetric target is given by:

$$\theta' = \arccos[\cos(\theta)\cos(\phi)] \quad (6)$$

where $\theta = \theta_o + \Delta\theta$, θ_0 is the target's aspect angle relative to the source, $\Delta\theta$ is the amount the ray is bent by horizontal reflection and refraction, and ϕ is the ray's angle with respect to the horizontal. The bistatic scattering approximation that will be discussed later is accomplished by letting $\theta = (\theta_i + \theta_j)/2$ and $\phi = (\phi_i + \phi_j)/2$. Doppler spreading of the signal due to interactions with a moving sea surface are not considered.

B. REVERBERATION

In general, boundary reverberation may be expressed as

$$R_{s,b}(f) = \int_{-\pi}^{\pi} \int_{0}^{\infty} \sum_{i} \sum_{j} X(f) B_S(f,\theta_i,\phi_i) H_i(f,\theta_i,\phi_i) \cdot \sigma_{ij}(f,\theta_i,\phi_i,\theta_j,\phi_j) H_j(f,\theta_j,\phi_j) B_R(f,\theta_j,\phi_j) r dr d\theta \quad (7)$$

where $B_{i,j}$ and $H_{i,j}$ have the same meaning as in Equation (5) and $\sigma_{i,j}$ is the scattering cross-section (per unit area). This equation applies to the ocean surface and bottom with the scattering cross-section determined as described in the following paragraph.

The ratio of incident to scattered intensities, as a function of f, θ_i, ϕ_i, θ_j, and ϕ_j, is given by Chapman and Harris, (1962), for surface reverberation and by Lambert's Law (Urick, 1983, p. 278) for bottom reverberation. These equations have been coupled with a three-dimensional boundary scattering function as described by Ellis and Crowe (1991), to account for scattering that occurs out of plane. This modification has a negligible effect on monostatic scenarios since the only change in the horizontal angle between incident and return paths is due to the horizontal components of reflection and refraction. The magnitude of σ ($= P_{scat}/P_{inc}$) is then just the square root of this intensity ratio. A random phaseshift is applied to each ray to account for uncertainties in the phase shift induced by the scattering and by fluctuations and uncertainties in the medium. Coherently summing all ray path combinations at each step of the integration, without introducing this random phase shift, produced results that did not represent realistic reverberation.

To implement the numerical integration of Equation (7), it is assumed that all terms except H_i and H_j are approximately constant over some small range Δr. Additionally, it is assumed that ray travel time is the only factor in the H_{ij}'s (which describe the set of eigenrays striking a region at range r_k) that varies over the interval Δr. The perturbated travel time for ray i,j over region Δr is approximated as

$$t_{i,j} = \frac{r - r_k}{c_{i,j} \cos(\theta_{i,j})} + t_{k_{i,j}} \tag{8}$$

and an analytical solution to

$$\int_{r_k}^{r_k+\Delta r} e^{-jw(t_i+t_j)} r dr \tag{9}$$

is used at each range step in the numerical evaluation of Equation (7).

To ensure that all rays striking a ring on the bottom are accounted for, the contour method of Franchi et al., (1984, pp. 8-11), was adopted. Their study involved calculation of the reverberation envelope as a function of time but they developed a method of characterizing families of rays based on number and type of boundary interactions and turning points in order to 'recognize' missed rays and interpolate between adjacent but similar rays to determine the ray parameters for each step in the numerical integration.

C. AMBIENT NOISE

Although spatial, temporal, and wind or traffic-induced variations in ambient noise levels were ignored for this study, it was desired to include ambient noise with a realistic frequency spectrum. To create an artificial ambient noise signal, an omnidirectional noise spectrum for the region of interest must be specified. This omnidirectional noise spectrum level (NSL) is then converted to the detected noise level (DNL) of the modelled array using the formula of Kinsler et al., (1982, p. 413):

$$DNL = NSL + 10\log w - DI \tag{10}$$

where w is the bandwidth of the modelled spectrum and DI is the array directivity index. The directivity index is computed from the formulas in Urick (1983, p. 43).

Once the magnitude of the ambient noise spectrum is obtained from Equation (10), a random phase is applied to each frequency component. The ambient noise signal is then the inverse fast Fourier transform of this complex spectrum.

III. CASE STUDY

To demonstrate the capabilities and potential usefulness of the modelling tools, a case study was performed. The Gulf of Sidra and the Barents Sea were chosen as the environments. An N by N billboard array was selected as the co-located source and receiver and a numeric model provided by Naval Research Laboratory was used as the target.

A. INPUTS TO CASE STUDY

1. Environment Simulation

For each region, the bathymetry database DBDB5, with 1/12 degree resolution, was used. CTD casts conducted during the Barents Sea Polar Front Experiment (Barents Sea Polar Front Group, 1992) provided the sound speed data for the Barents Sea. For the Gulf of Sidra, output from the Coastal Ocean Circulation Model of Ly et al., (1994) was used. This model provided temperature and salinity along scaled depth levels, which were converted to sound speed using the formula of Clay and Medwin (1977, p. 3).

Sound speed and bathymetry data were gridded and formatted for HARPO as described by Mykyta (1993). Horizontal interpolation of sound speed and bathymetry was used to fill in their respective grids. The gridded data were converted to continuous fields by routines that have been incorporated with HARPO, (see

Newhall et al., (1987), Chiu et al., (1994a), and Chiu et al., (1994b)). Note that although virtually any resolution of sound speed or bathymetry data could be used, the data fields used in the present examples had resolutions not much better than the target ranges studied, hence the modelled environments are only weekly three-dimensional.

The first results that will be presented are for a roughly 750 m deep region in the Gulf of Sidra. Some results for a 1500 m region in the Gulf of Sidra as well as a 285 m deep region in the Barents Sea will also be presented. Representative sound speed profiles for these regions can be seen in Figure 1.

For the Gulf of Sidra, a bottom density of 1430 kg/m^3 and a bottom sound speed of 1750 m/s were used. For the Barents Sea, these parameters were 2600 kg/m^3 and 3000 m/s, respectively. For both cases, an rms roughness of 0.5 m was assigned to the surface and bottom. A value of -38 dB was used for Lambert's constant in the computation of reverberation signals. These values are somewhat arbitrary but chosen to be similar to values appearing in various other studies.

2. NRL Target Model

The Naval Research Laboratory has provided a tabulated model of the far field, plane wave scattering from a hemispherically end-capped steel cylindrical shell immersed in water. The cylindrical section is 100 meters long with a diameter of five meters and wall thickness of five centimeters. The (complex) transfer function is the ratio of the scattered pressure referenced to one meter from the acoustic center of the target to the incident pressure at the target's location:

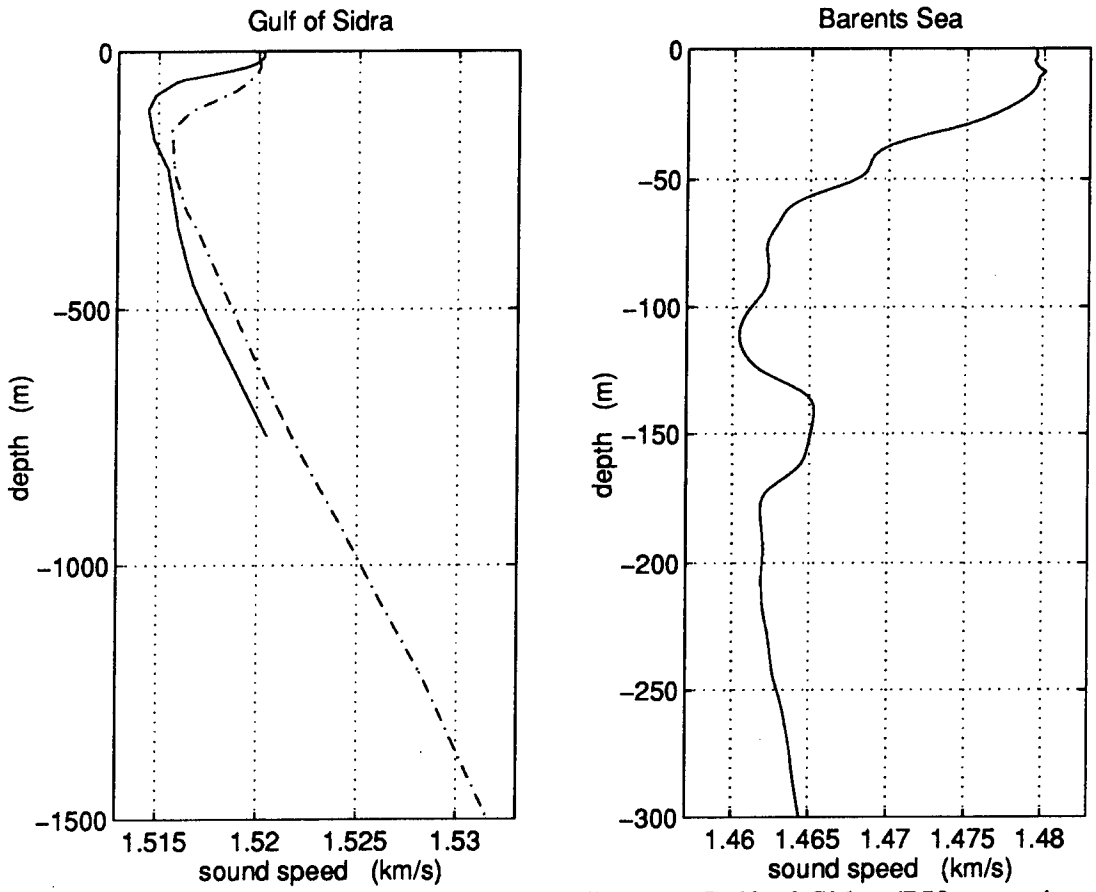

Figure 1. Representative Sound Speed Profiles (a) Gulf of Sidra (750 m region: solid line; 1500 m region: dash-dot) and (b) Barents Sea.

$$\sigma_t(f,\theta) = \frac{P_{scat}(f,\theta)}{P_{inc}(f,\theta)} \tag{11}$$

The monostatic scattering angle, θ, is the angle relative to the z-axis, which is aligned with the axis of the cylinder. Data have been provided for monostatic scattering as a function of incident angle and frequency for frequencies from 100 to 290 Hz at a frequency resolution of one-half Hz and angular resolution of

one degree. With this definition of σ [1], the frequency and aspect dependent target strength is given by:

$$TS = 20\log|\sigma_t| \tag{12}$$

Figures (2a) and (2b) provide examples of the frequency and aspect dependence of target strength for the NRL model. The example of frequency dependence shown is

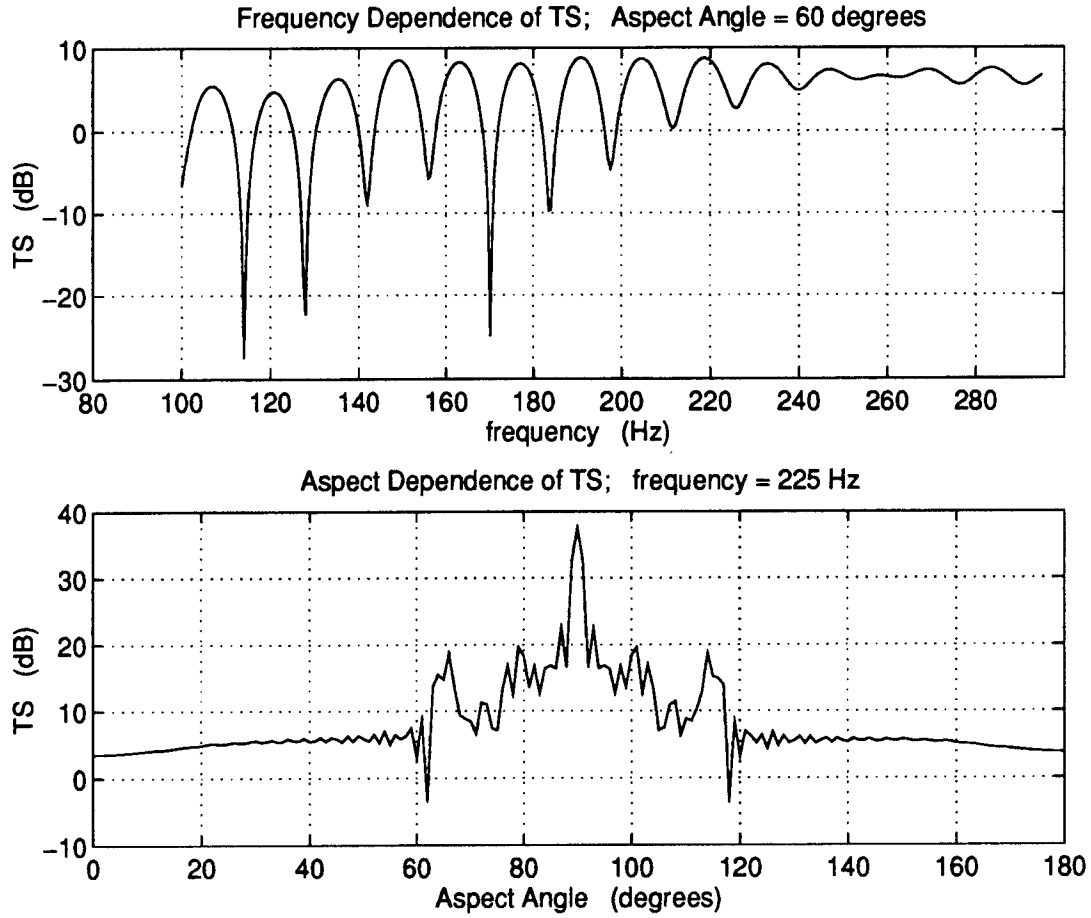

Figure 2. Target Strength of NRL Model: (a) Frequency Dependence at 60 Degrees Aspect Angle and (b) Aspect Dependence at 225 Hz.

[1] Note that σ is proportional but not identical to the form function, f_∞, often used in acoustic scattering studies. For plane waves, σ is related to S, the far field scattering function described by Ingenito (1987), by $\sigma = -j\rho_0 cS$.

for an aspect angle of 60 degrees and the example of aspect dependence is for a frequency of 225 Hz.

Investigations were limited to the frequency band of the NRL model but the purely monostatic nature of the model placed further restrictions on the present study. Even with the source and receiver co-located, a target in a channel is ensonified by multiple paths, (see Figure (8), appearing later). To provide an estimate of the contribution from this 'bistatic' scattering, the approximation described by Urick (1983, pp. 302-306), was used. According to this approximation, developed for radar applications, the bistatic target strength is equal to the monostatic target strength taken at the bisector of the bistatic angle. While this approximation will make it possible to use the NRL target model, it is not expected to be a very accurate approximation of the acoustic scattering from an object when the wavelength is not considerably smaller than the features of the target. Hence it will be a source of error in the final results [2].

3. Active System Configuration

The monostatic system consists of a two-dimensional array of elements, arranged in N rows by N columns, evenly spaced by a distance d. This provides both vertical and horizontal directionality. Not only does this directionality aid in reducing reverberation and detected ambient noise, it can mitigate some of the errors due to the 'bistatic' scattering approximation discussed above.

---

[2] Given a bistatic target model, xfer.m will compute the received echo for a bistatic scenario, using the raypaths from two different runs of HARPO, without the need for this bistatic approximation.

The vertical or horizontal beam factor of the "billboard" array as a function of the off-axis angle, θ, is given by Kinsler et al., (1982):

$$b(\theta) = \left| \frac{1}{N} \frac{\sin[\frac{N}{2} kd(\sin\theta - \frac{c\tau}{d})]}{\sin[\frac{1}{2} kd(\sin\theta - \frac{c\tau}{d})]} \right| \qquad (13)$$

where

k = *the wave number* $(2\pi/\lambda)$
N = *number of rows or columns of array elements*
d = *element separation*
c = *local sound speed*
τ = *sequential time delay used for array steering*

By applying a sequential time delay (i.e., a linear phase shift) to the elements in each row, the array can be steered vertically by an angle given by:

$$\sin\theta_0 = \frac{c\tau}{d} \qquad (14)$$

To obtain a reasonable compromise between the desire to minimize beamwidth and the desire to minimize the size of the secondary lobes, N was chosen to be 5 and d was chosen to be 4 meters. This makes for a sizeable array. Any complications in deployment or due to array element interactions have been ignored. A cross-section of the beam pattern can be seen in Figure 3 at a frequency of 225 Hz. Horizontal and vertical beam patterns are identical.

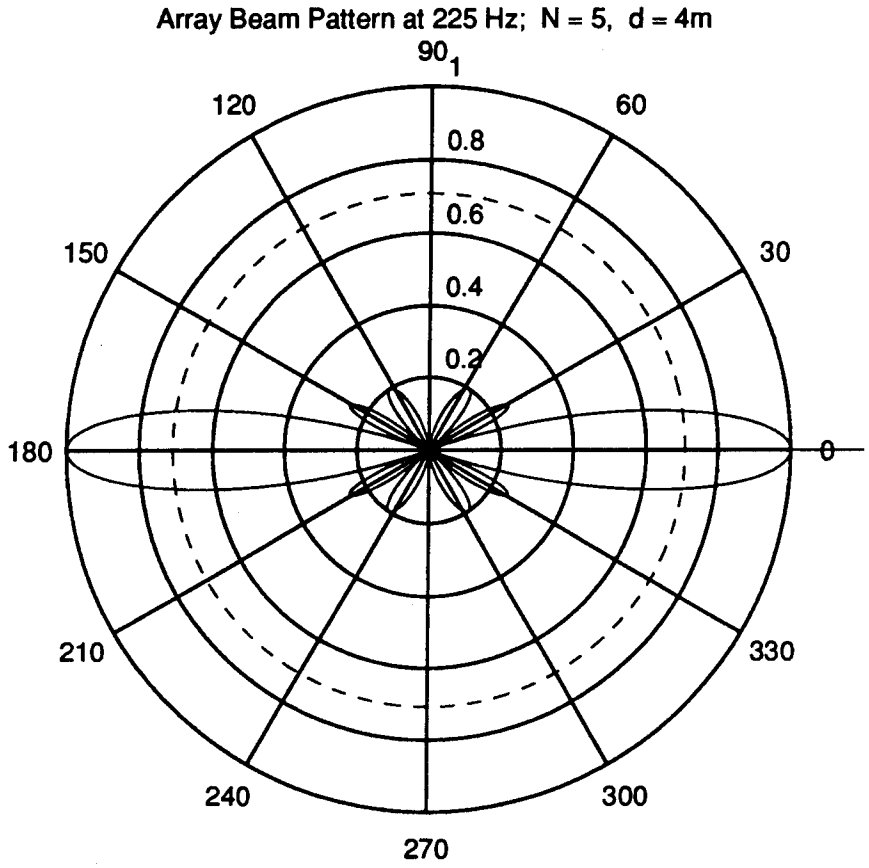

Figure 3. Beam Pattern of Transmit/Receive Array at 225 Hz.

4. Transmitted Signal

The choice of transmitted signal will not only affect the target echo, but reverberation as well. Several factors must be considered. The signal must, of course, be within the technical constraints of the transmitter, receiver, and signal processing equipment. Additionally, a broadband signal may provide more information about the frequency dependence of the target's echo but reduces the possibility of doppler separation between echo and reverberation. A narrower banded signal cuts down the amount of frequency information but allows the use of doppler separation and may also allow the mapping of nulls in a target's aspect dependent scattering, (via a multi-

static scenario), as a means for identifying resonances. Several experimental methods that have been used to identify the resonances of submerged acoustic scatterers are discussed in Pierce and Thurston (1992 and 1993).

A gaussian-weighted, linear-frequency-modulated (GLFM) pulse was selected for this case study due to it's relatively smooth spectrum. A sample of this pulse and its FFT can be seen in Figures 4 (a) and 4 (b). The parameters of this pulse

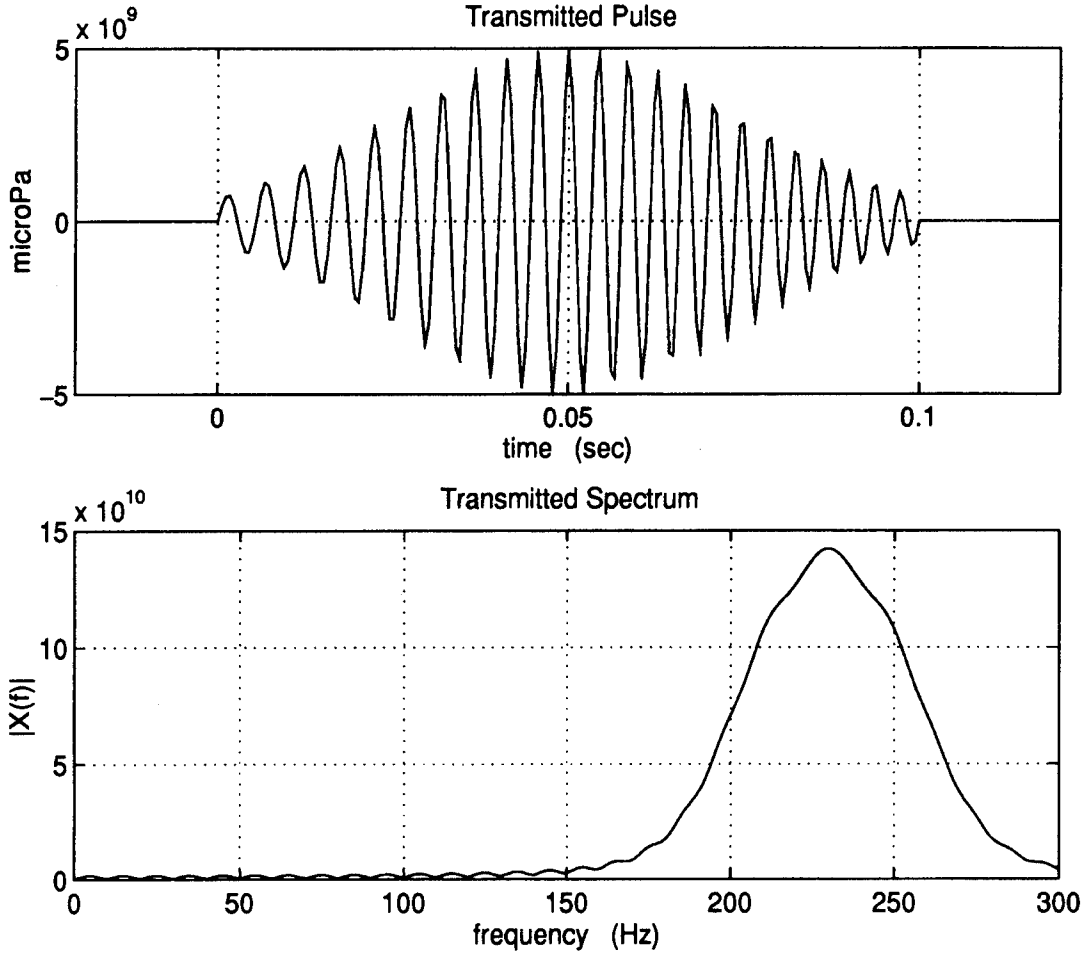

Figure 4. (a) GLFM Pulse (b) FFT of the GLFM Pulse.

are: length 0.1 seconds, initial frequency 180 Hz, final frequency 230 Hz, Gaussian weighting factor 800 sec^{-2}, and peak-to-peak source level of 200 dB re 1 microPascal.

B. RESULTS AND ANALYSIS OF CASE STUDY

The examples that follow will be based on a target aspect angle of 60 degrees and the transmitted GLFM pulse of Figure 4. Figure 5 shows the impulse response of the NRL modelled target at 60 degrees as well as the target transfer function's magnitude and phase. Notice the nulls and peaks in Figure 5 (b); we will be looking for these later in the modelled echos.

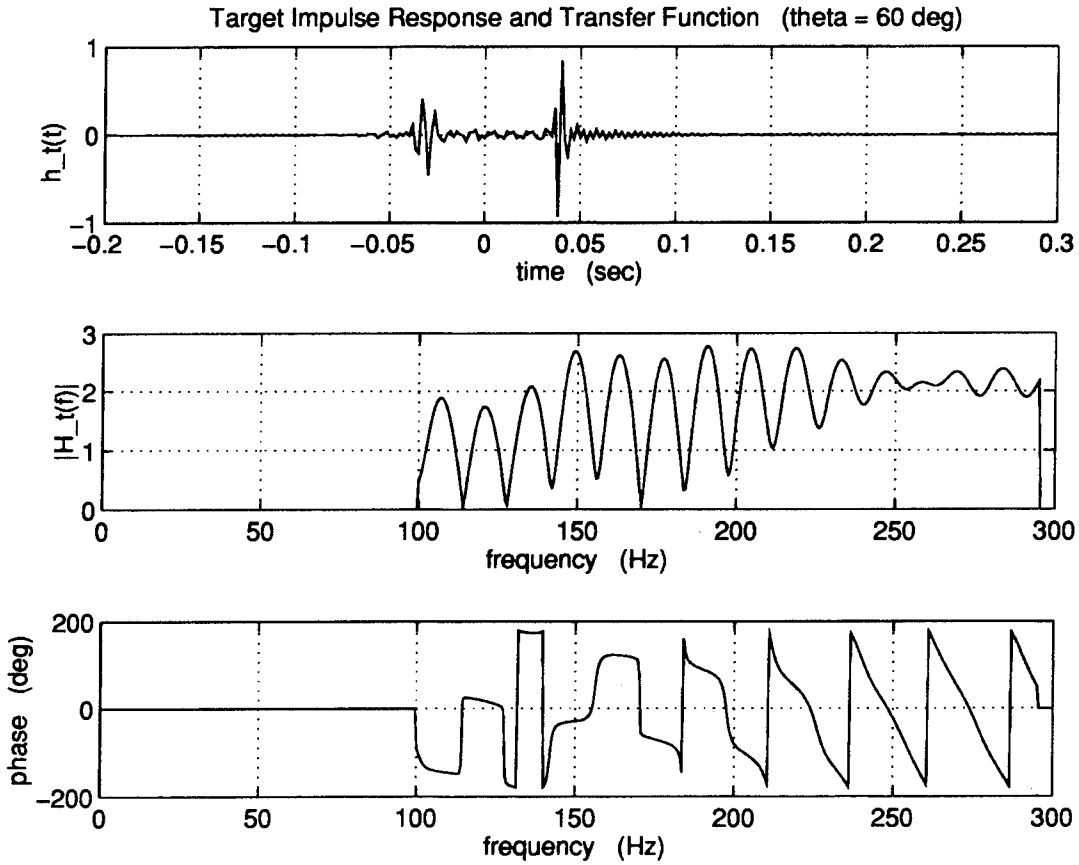

Figure 5. NRL Target Model at 60 Degrees Aspect Angle: (a) Impulse Response, (b) Magnitude of Transfer Function, and (c) Phase of Transfer Function.

Figure 6 shows what the ideal echo would look like with all environmental factors ignored [3]. In this case, the received signal is

$$Y(f) = X(f) \cdot \sigma_t(f, 60°) \tag{15}$$

and the spectrum of Figure 5 (b) can be seen superimposed on the spectrum of Figure 3 (b).

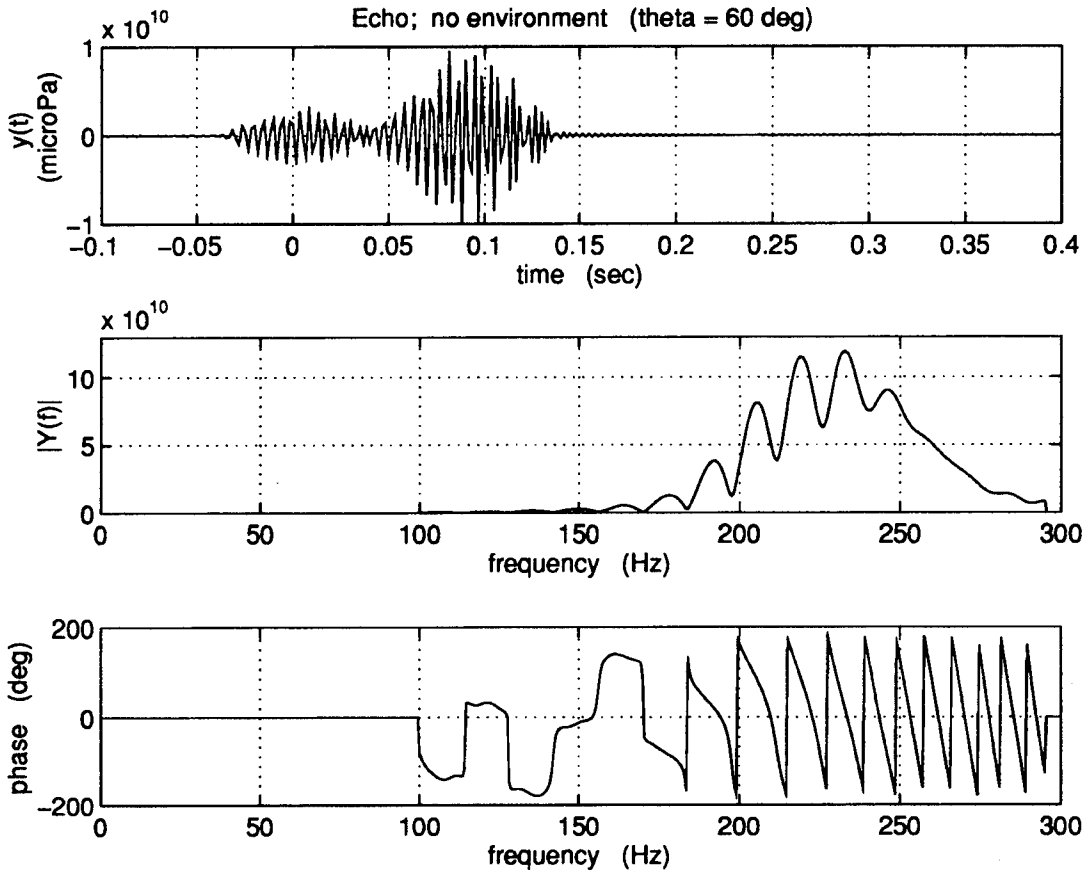

Figure 6. Ideal Target Echo With All Environmental Effects Ignored: (a) Echo, (b) Magnitude of FFT, and (c) Phase of FFT.

[3] This is the "reference" signal that will be mentioned and used later.

To create an ambient noise signal, the shallow water spectrum of Gordon Wenz' classic paper (Wenz, 1962) was used. The resulting ambient noise spectrum and signal can be seen in Figures 7 (a) and 7 (b). The ambient noise signal in Figure 7 (b)

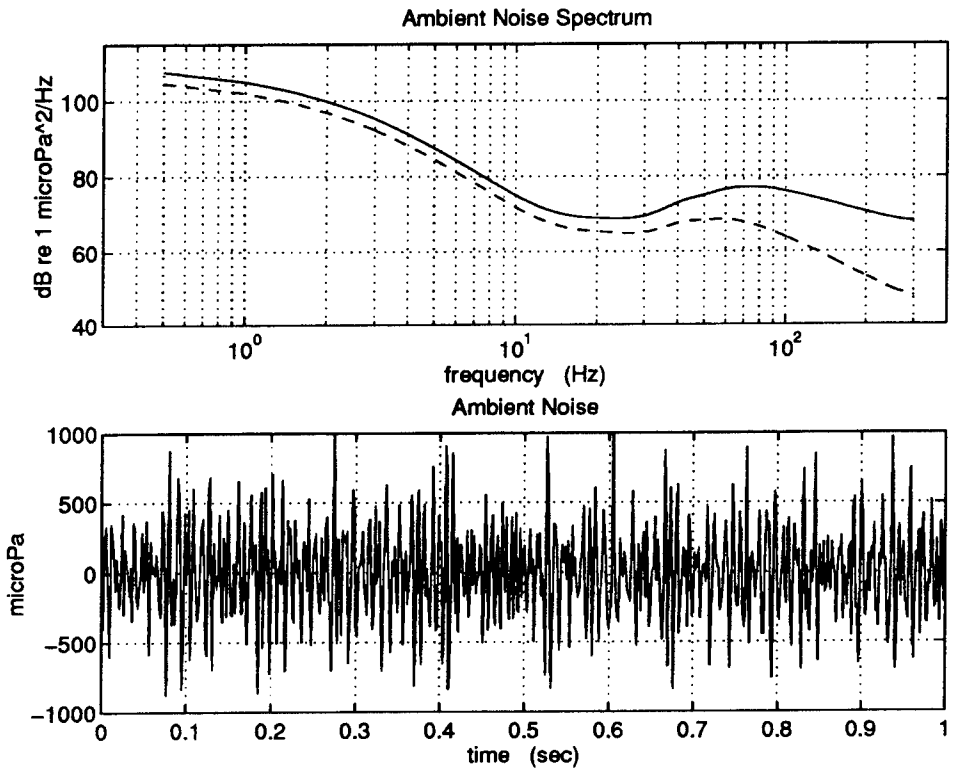

Figure 7. Simulated Ambient Noise: (a) Spectrum and (b) Signal. The solid line in Figure 7(a) is the NSL from Wenz (1962) and the dashed line is the DNL.

has been band-pass filtered with a fourth order Butterworth filter having lower and upper pass frequencies of 100 and 290 Hz, respectively. Noise from the sea surface arrives predominately from the vertical while shipping noise arrives predominately

from the horizontal. These effects were neglected but would tend to increase shipping noise and decrease wind noise from the levels determined above for the modelled array.

The signal modelling program computes a signal in the frequency domain for frequencies from -300 to +300 in 0.5 Hz increments. The IFFT of this result is the received signal, which is then a two second long time series with a 600 Hz sampling frequency.

The reference echo introduced in the last section was used to quantitatively analyze the distortion of the echo induced by the channel. The method of comparison was a crosscorrelation between a windowed portion of the modelled signal and this reference signal. To further illuminate the impact of the oceanic channel on the prospect of active classification, a false target having a frequency and aspect independent target strength was also modelled. This allowed a comparison of the distorted "appearances" of the two targets.

The modelled signal consists of a string of multipath arrivals, some of which overlap. Crosscorrelating the entire signal with the reference signal was not helpful due to this multiple arrival structure. A more illuminating method that can easily be implemented, and the one used in the results that follow, was to apply a 256 point hanning window (approximately 0.4 seconds wide) to the signal, centered on the first arrival. Due to various factors that will be illuminated in the sections that follow, windowing on the first arrival gave the highest peak in the crosscorrelation for nearly all cases.

1. Gulf of Sidra (750 m region)

Figures 8 through 10 are based on a source/receiver depth of 60 meters and a target depth of 60 meters in the shallow Gulf of Sidra region. The range to the target was varied from 5 to 10 km and, as previously mentioned, the target's aspect angle is 60 degrees. Figure 8 shows some examples of eigenray families for the target at three different ranges. Beyond 7 km, there were no refracted (RRR) or refracted/surface-reflected (RSR) paths and the first arrival was due to a

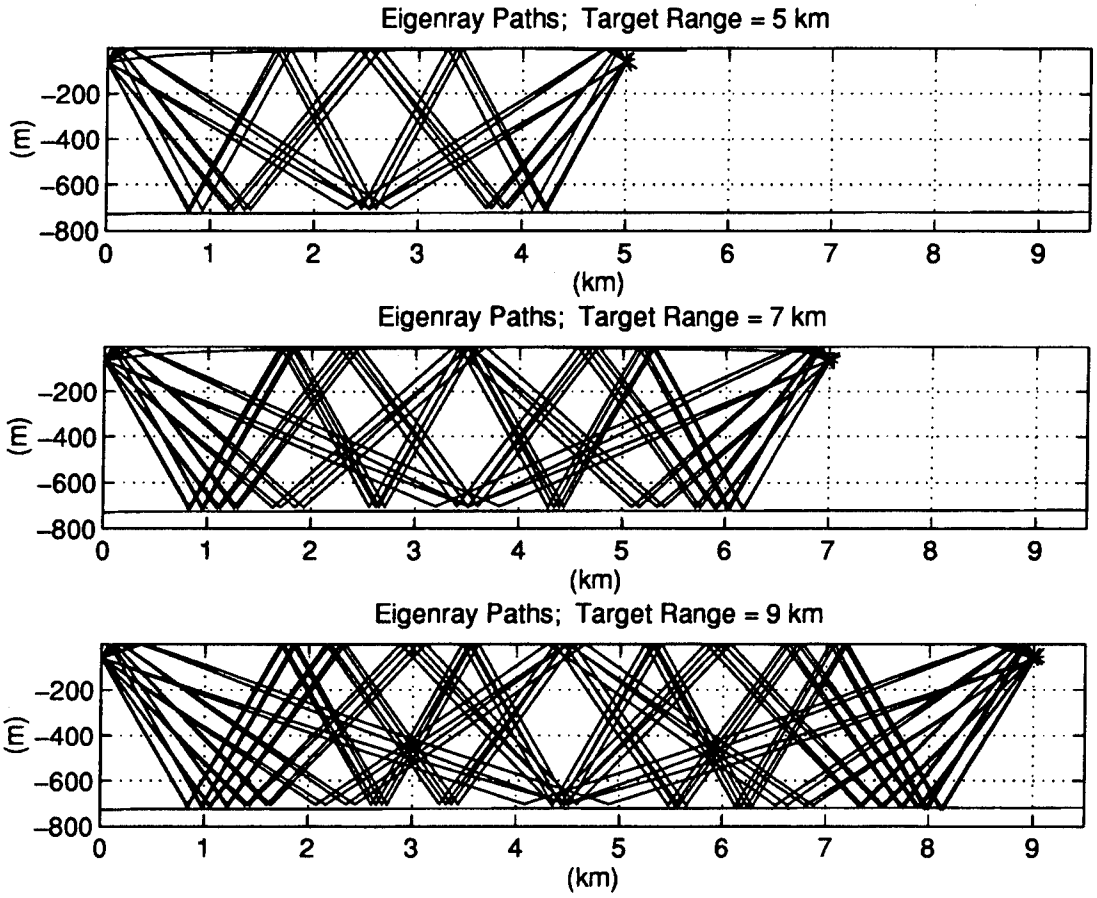

Figure 8. Eigenray Paths for Target Ranges of 5, 7, and 9 km.

refracted/bottom-reflected path (RBR). Due to the shallow array and target depths, batches of surface-reflected/bottom-reflected (SRBR) and RBR paths have similar travel times. At greater ranges, the grazing angles for equivalent families of rays get shallower. In general, fewer or shallower boundary interactions for a ray result in less distortion but overlapping arrivals degrade the signal. The arrival structure for shallow water regions such as this is dominated by bottom depth and slope rather than by refraction.

Figure 9 is the simulated echo for a target range of 5 km along with a plot of the eigenray launch angles and travel times [4]. Sequential arrivals at the source correspond to combinations of ray paths connecting the source and target and the target and receiver. Since we are concerned here with a monostatic scenario, the first arrival corresponds to two-way travel on the shortest path. The first arrival in Figure 9 provides a relatively clean echo but subsequent arrivals begin to overlap. Later arrivals become significantly distorted due to overlapping travel times and more or steeper boundary interactions.

For Figure 9 and all further results, the transmit/receive array's beam pattern was oriented horizontally and not steered to enhance the earliest arrival. It was found that this did not have a significant impact on the crosscorrelation analysis applied to analyze the multi-path affects. Beam steering will, however, aid in signal

[4] Ray travel times have been normalized by subtracting the travel time of the earliest arrival.

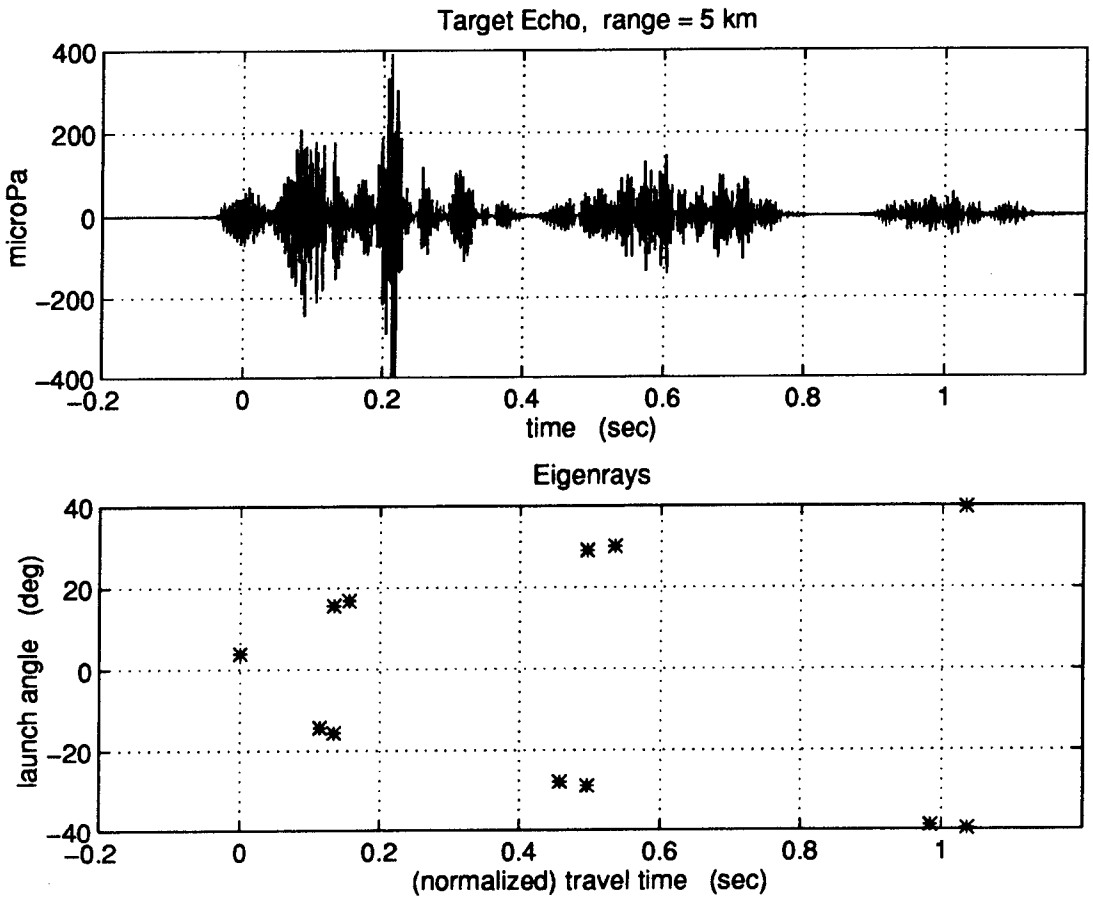

Figure 9. (a) Simulated Echo, (b) Eigenray Launch Angles vs. Travel Times.

detection and recognition when noise and reverberation are present by providing roughly 1 to 3 dB increase in the signal.

In Figure 10, the modelled echos for target ranges of 5 to 10 km can be seen. At 5, 6, and 7 km, the initial portion of the echo results from a path that is free of boundary interactions and strongly resembles the reference echo of Figure 6 (a). The distortion grows as separation decreases or boundary interactions become more significant.

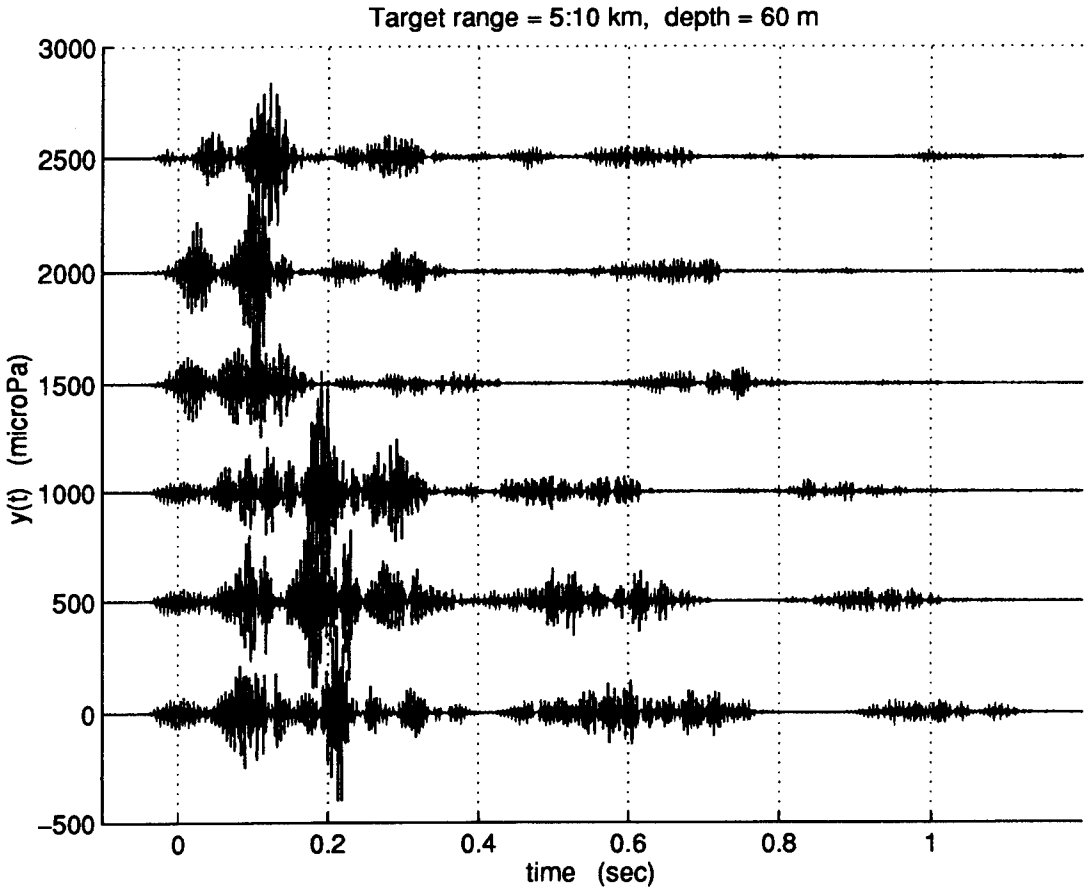

Figure 10. Simulated Echos for Target Ranges of 5 to 10 km, Target Depth 60 m. The 5 km echo is at the bottom.

Figure 11 is an analysis of the spectra of the windowed section of each of the echos from Figure 10. As discussed earlier, the window is approximately 0.4 seconds wide and centered on the first arrival. The solid line is the echo from the NRL target, the dotted line is the reference echo (NRL target with no environment), and, for comparison, the dash-dotted line is the echo from a frequency independent false target. The spectra have been normalized for ease of comparison. At shorter ranges, it would be very difficult to distinguish between the false target and the NRL

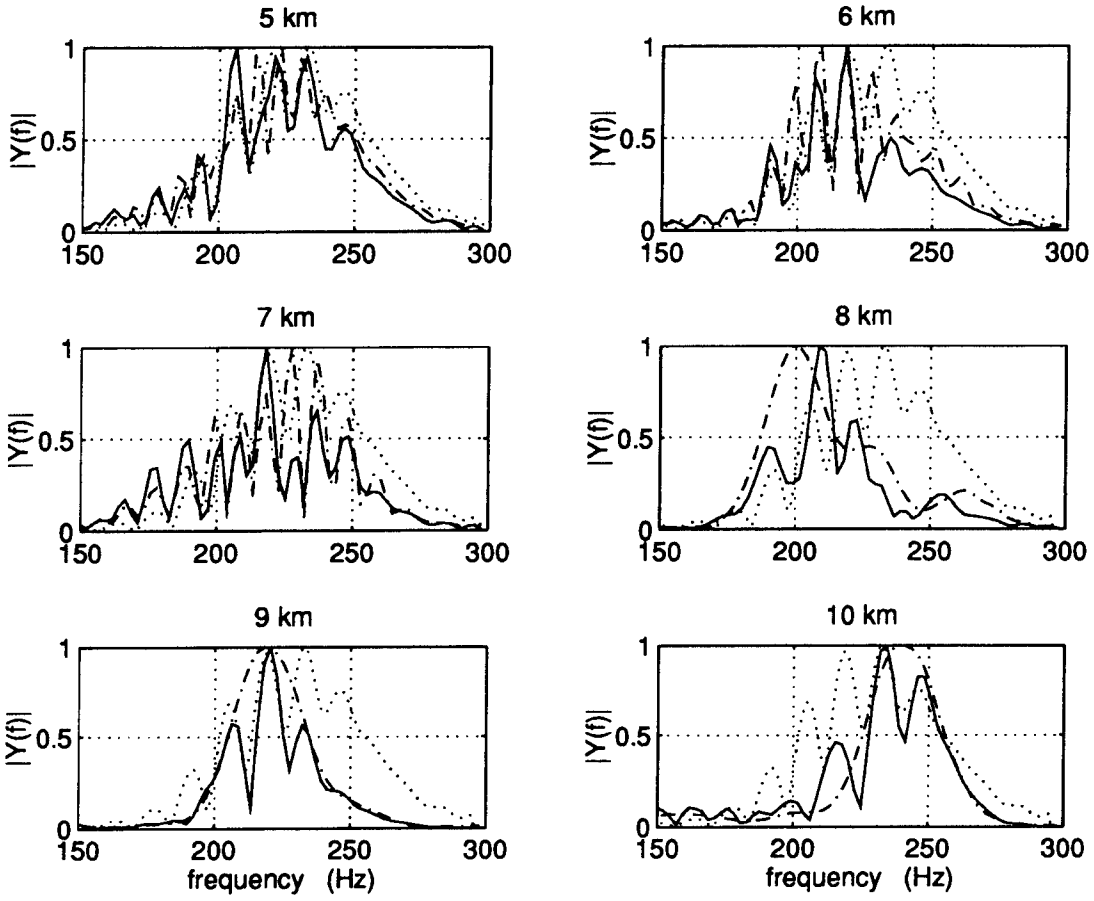

Figure 11. FFT's of Windowed Signals for Various Target Ranges; NRL Target (solid line), False Target (dash-dotted), Reference Echo (dotted line).

target. At greater ranges, the spectra of the two targets begin to show quantifiable differences, with the NRL target's spectrum displaying nulls and peaks that can only be attributed to the target.

Peaks in the crosscorrelations between the windowed signals and the reference echo are plotted in Figure 12 for the NRL target and the false target. Notice the change in the trend at 8 km, when the propagation mode of the dominant early arrival has changed from RRR or RSR to RBR.

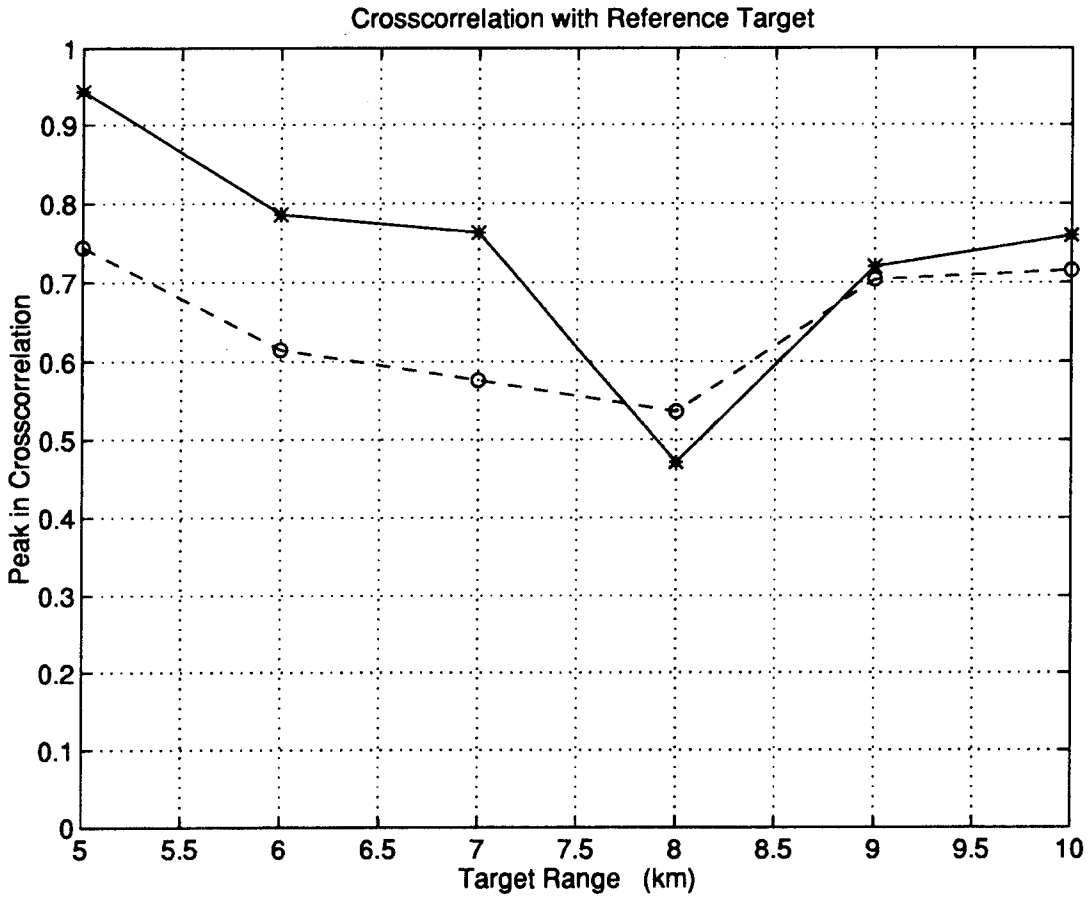

Figure 12. Crosscorrelation Peaks as a Function of Target Range; NRL Target (solid line), False Target (dashed line).

Figure 13 is similar to Figure 12 but displays the results for various source/receiver array depths operating against the NRL target. The trends are similar for array depths of 60, 90, and 120 m. But for an array depth of 30 m, there is no purely refracted path connecting the array and the target at any of the plotted ranges.

The impact on the modelled echo of variations in target depth is illustrated in Figure 14, for target depths of 20 to 180 m at 40 m increments. Figure 15 contains the spectra of the windowed signals from the NRL target echos of Figure 14 as well

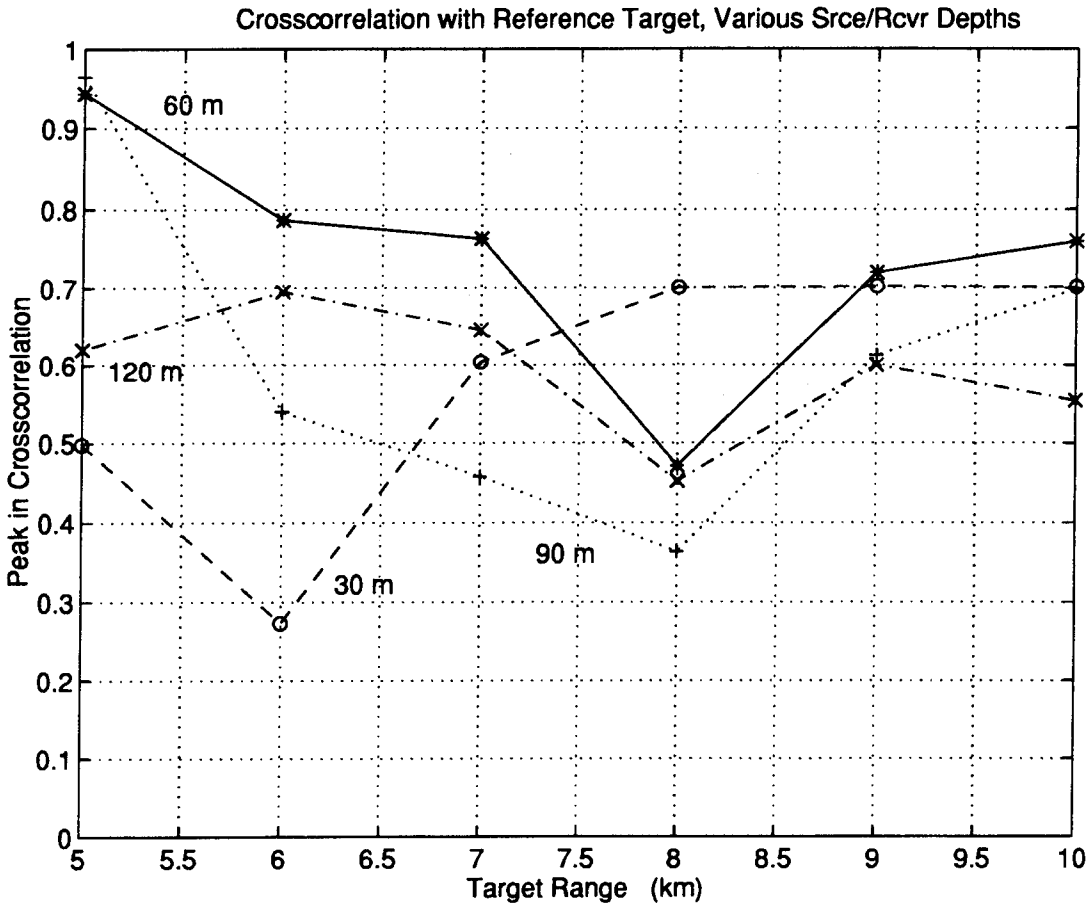

Figure 13. Crosscorrelation Peaks as a Function of Range for Various Source/Receiver Depths.

as from the false target at each location. Again, the spectrum of the reference echo is plotted for comparison.

Figure 16 is an analysis of the impact of reverberation and ambient noise on the crosscorrelation of the windowed signal with the reference echo. The results of Equation (7) for reverberation were validated by comparing the reverberation level in the computed signals for a CW pulse to the reverberation level estimation formulas in Urick (1983, p. 245) and the results were found to be consistent. For the GLFM pulse, signal to reverberation levels in the cases studied were typically -15 to -20 dB.

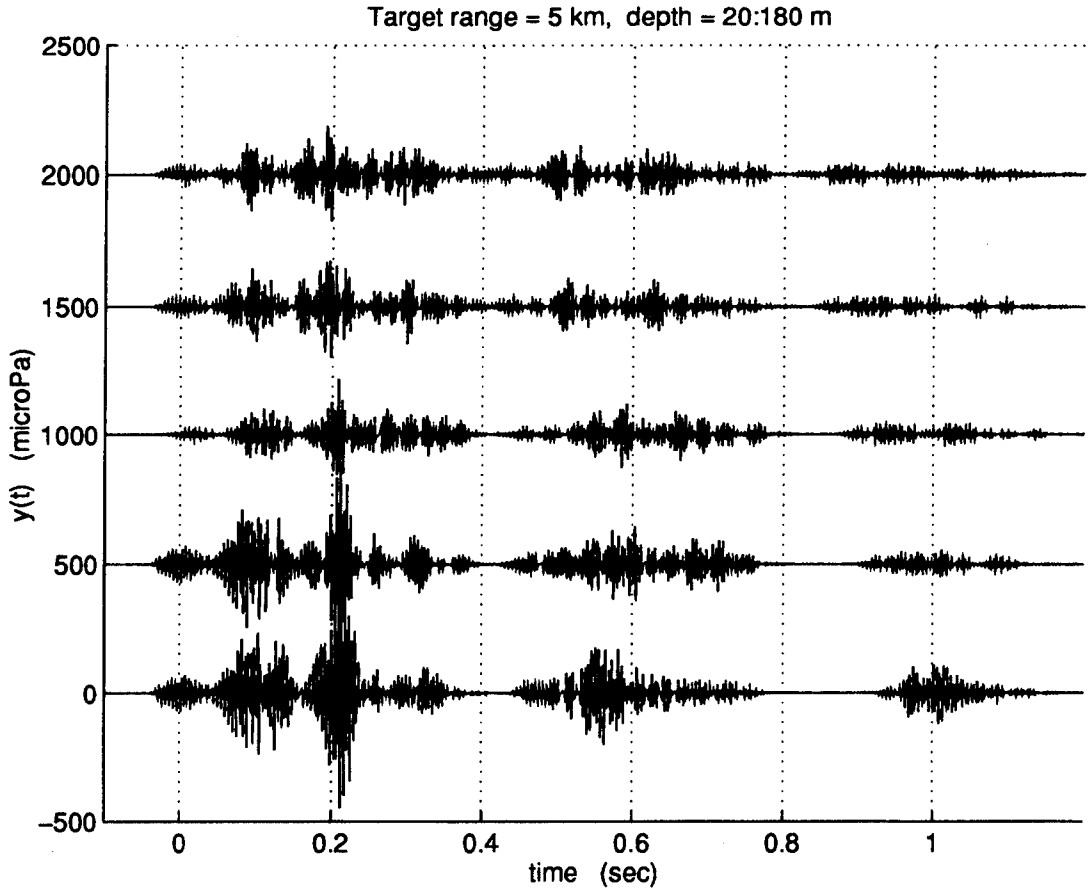

Figure 14. Simulated Echos for Target Depths of 20 to 180 Meters, Range = 5 Kilometers. The echo for a target depth of 20 meters is at the bottom.

Ambient noise was typically 5 to 10 dB above the signal. In Figure 16, reverberation level and ambient noise level were parameterized to see their impact on signal crosscorrelation. As SNR or SRR decreases, the crosscorrelations drop, reaching a valley by about -10 dB, independent of target type.

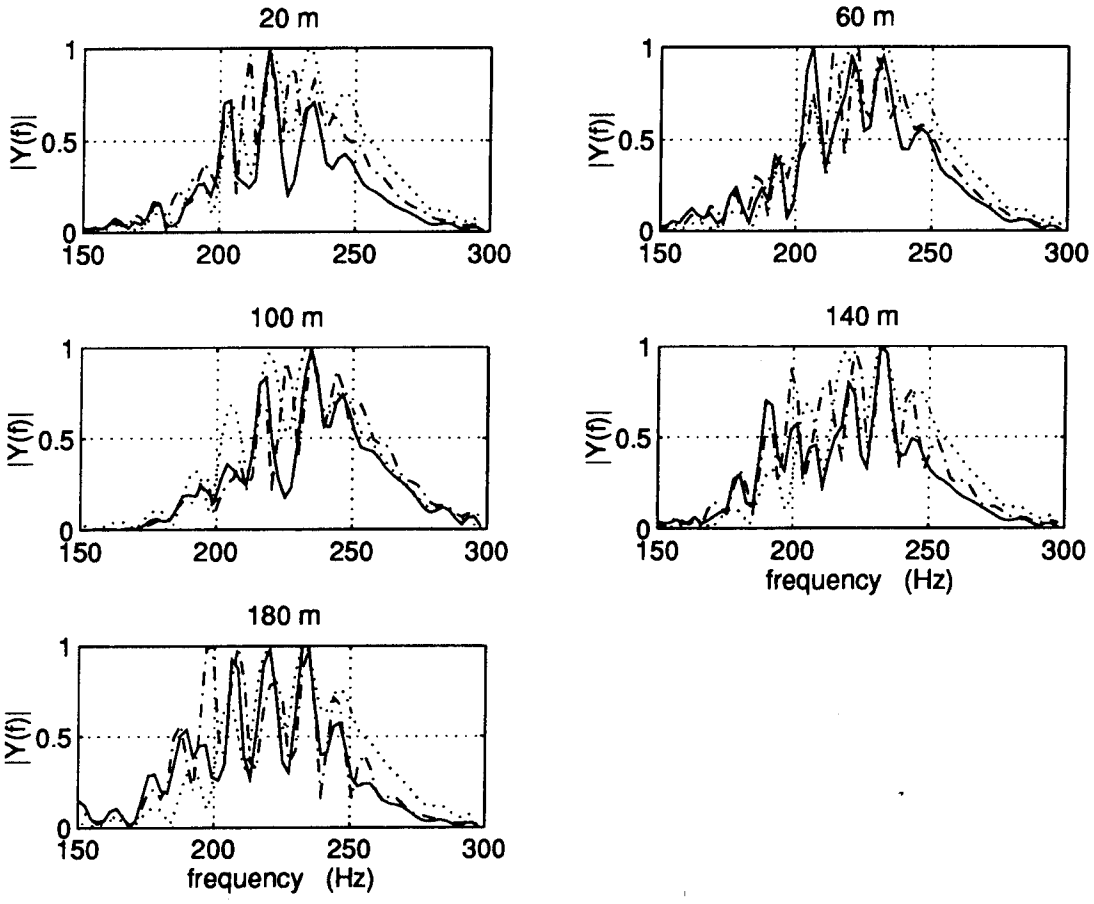

Figure 15. FFT's of Windowed Signals for Various Target Depths; NRL Target (solid line), False Target (dash-dotted), Reference Echo (dotted line).

2. Gulf of Sidra (1500 m region) and Barents Sea

For comparison with the results of the previous section, some results for two different regions will be presented here. In Figure 17, the spectra of windowed echos for a 1500 meter deep area in the Gulf of Sidra have been plotted. All parameters are identical to the conditions of Figure 11 except the bathymetry and the sound speed field. Classification of the NRL target and the false target can be readily made at each range.

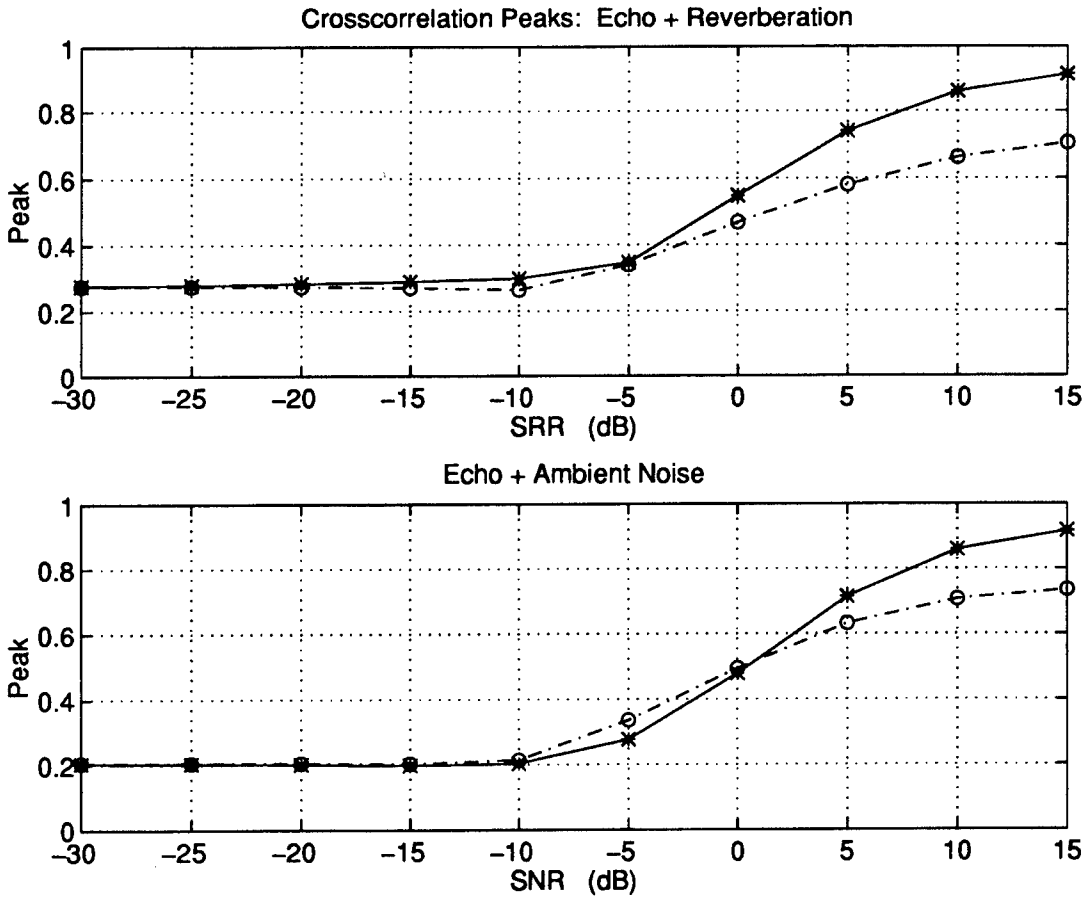

Figure 16. Crosscorrelation Peak vs. SRR and SNR, NRL Target (solid line), False Target (dash-dot): (a) Echo + Reverberation, (b) Echo + Ambient Noise.

Figure 18 presents the results for the 285 meter deep Barents Sea region. Here, both targets are difficult to recognize. For this area, bathymetry, sound speed field, and bottom density and sound speed are different. Figure 19 displays the trends in crosscorrelation peaks for the two regions just discussed.

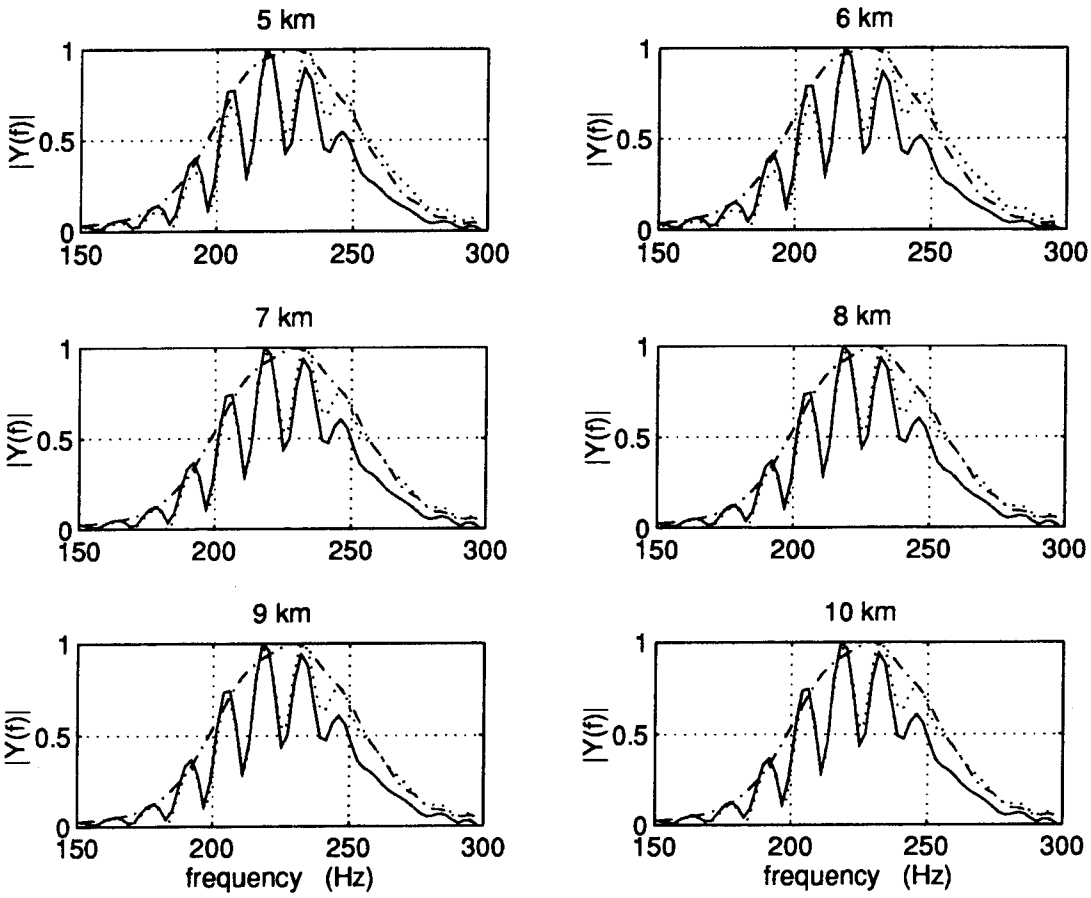

Figure 17. FFT's of Windowed Signals for Various Target Ranges (Gulf of Sidra); NRL Target (solid line), False Target (dash-dotted), Reference Echo (dotted line).

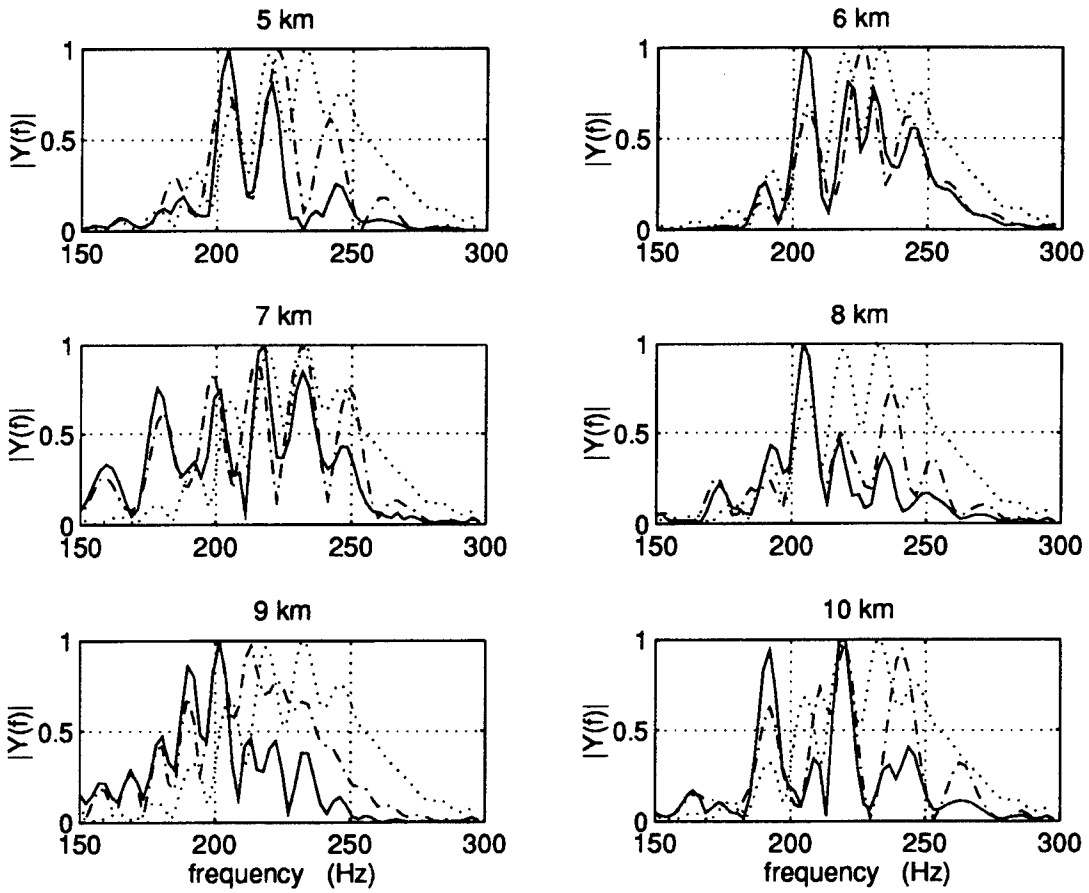

Figure 18. FFT's of Windowed Signals for Various Target Ranges (Barents Sea); NRL Target (solid line), False Target (dash-dotted), Reference Echo (dotted line).

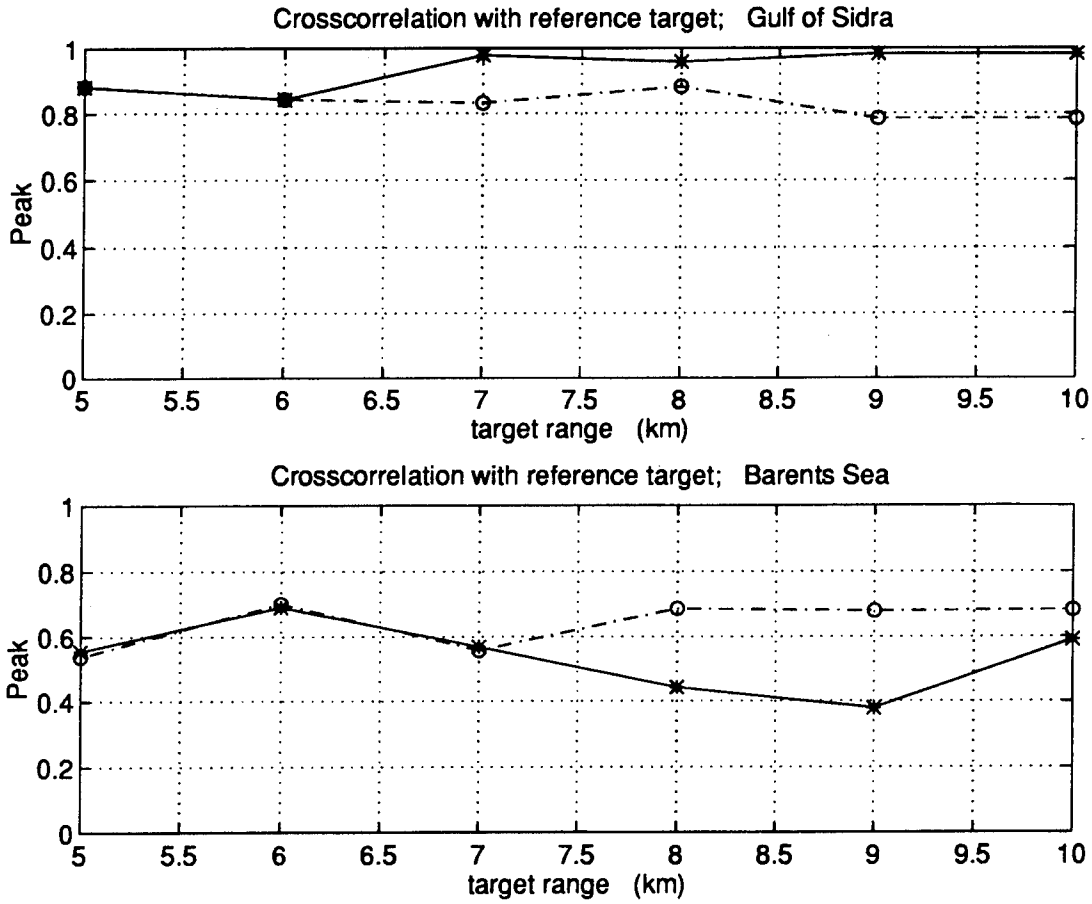

Figure 19. Crosscorrelation Peaks as a Function of Target Range; NRL Target (solid line), False Target (dashed line), (a) Gulf of Sidra (1500 m region), (b) Barents Sea.

V. CONCLUSIONS

Tools for modelling the echo from a target in an arbitrary ocean environment have been developed and successfully applied to the Barents Sea and the Gulf of Sidra. The programs are quite adaptable and can be used to evaluate the performance of any system or signal against any target. These components are simply entered into the modelling programs in the form of MATLAB functions.

Although only one system was considered in the case study, some implications for active classification were apparent. The multipath arrival structure and distortion induced by boundary interactions make classification with conventional signal processing techniques much more difficult. Isolating individual paths and using matched-filter techniques to account for the distortion induced by boundary interactions may be helpful. In addition to the difficulty of extracting an echo from a received signal contaminated by noise and reverberation, signal processing techniques must account for the influence of the environment.

Although it may be possible to boost source level to gain an advantage over ambient noise, this method does not work if conditions are reverberation limited. Equation (11) provides a transfer function for boundary reverberation. With a single computation, Equation (9) provides a transfer function for the oceanic channel with a target in place that can be used with any transmitted pulse, X(f), as long as the target is considered stationary. If the target is moving, then the assumption of linearity

among the various ray paths does not apply and it is necessary to recompute Equation (9) for each transmitted pulse. Once computed, these results for the target echo and for boundary reverberation can quickly be combined with various pulse types, allowing determination of a pulse that optimizes target classification.

Averaging over several pulses, a technique commonly used to reduce random noise, may not work in practice due to pulse-to-pulse fluctuations in the environment and the fine time-frequency resolution required to resolve target characteristics. It may be necessary to consider a time-varying matched filter. Small changes in environmental parameters can significantly alter the structure of the received pulse. It may not be practical or possible to measure and model in-situ conditions accurately enough.

VI. RECOMMENDATIONS FOR FURTHER STUDY

Future work could involve experimenting with different systems and signals to optimize classification prospects. The output from these programs can also be used to test classification algorithms or as the basis for matched-field processing. Since ray-based modelling was used, the frequencies can readily be scaled for a transition from submarine-sized objects to mine-sized objects. Mine hunting as well as anti-submarine warfare is plagued by false alarms. An autonomous underwater vehicle with the ability to quickly distinguish between valid and false targets would be an extremely valuable asset.

With a fully bistatic target model, bistatic and multi-static scenarios could be studied. Receivers at more than one aspect angle could aid in mode identification by mapping the aspect dependence of scattering at particular frequencies.

The impact of fluctuations and variability of the medium, due to currents, internal waves, turbulence, biologics, etc., could be modelled. One approach would be to perturb the amplitude and phase of each frequency component in the ray-path transfer function. Various phenomenon could be assigned their own statistics, frequencies, and scales of variability. One could also perform multiple HARPO runs, treating the sound speed field as a function of time as well as space to study the magnitude of the impact of variability. Modifications to the modelling scheme could

also incorporate site and environmental dependence of ambient noise. See, for example, Ingenito and Wolf (January, 1989) and Perkins et al., (1993).

An interesting and ultimately necessary test of the validity of the computations in this paper and of active classification in general is to perform an experiment. A scaled-down channel and a scaled-down target could be used with appropriately scaled frequencies. Sand and/or clay could be used for the bottom with objects of various shapes, sizes, and rigidity used for targets. Surface roughness could be provided by a fan blowing over the surface. The target transfer function could be theoretically or empirically derived (i.e., by measuring the scattered field while taking steps to reduce the impact of the environment). Target echos with the target in the channel could then be measured and compared to the signals predicted using the above methods.

LIST OF REFERENCES

Barents Sea Polar Front Group (R. Bourke, C.-S. Chiu, J. Lynch, J. Miller, R. Muench, and A. Plueddemann), "Preliminary Cruise Results: Barents Sea Polar Front Experiment," unpublished, August 1992.

Brekhovskikh, L. M., *Waves in Layered Media*, Academic Press, New York, 1980.

Brekhovskikh, L. M. and Y. Lysanov, *Fundamentals of Ocean Acoustics*, Springer-Verlag, New York, 1982.

Chapman, R. P., and J. H. Harris, "Surface Backscattering Strengths Measured with Explosive Sound Sources", *J. Acoust. Soc. Am.*, 34(10), pp. 1592-1597, October 1962.

Chestnut, Paul, Helen Landsman, and R. W. Floyd, "A sonar target recognition experiment", *J. Acoust. Soc. Am.*, 66(1), pp. 140-147, July 1979.

Chiu, C.-S., A. J. Semtner, J. H. Ort, and J. H. Miller, "A ray variability analysis of sound transmission from Heard Island to California", *J. Acoust. Soc. Am.*, 1994a (in press).

Chiu, C.-S., J. H. Miller, and J. F. Lynch, "*Inverse Techniques for Coastal Acoustic Tomography*", in Environmental Acoustics, (D. Lee and M. Schultz editors), World Scientific, 1994b (in press).

Clay, C. S. and H. Medwin, *Acoustical Oceanography: Principles and Applications*, John Wiley & Sons, New York, 1977.

Eller, A. I. and L. Haines, *Identification and Acoustic Characterization of Seamounts*, SAIC-87/1722, Science Application International Corporation, McLean, VA, 1987.

Ellis, D. D. and D. V. Crowe, "Bistatic reverberation calculations using a three-dimensional scattering function", *J. Acoust. Soc. Am.*, 89(5), pp. 2207-2214, May 1991.

Franchi, E. R., J. M. Griffin, and B. J. King, *NRL Reverberation Model: A Computer Program for the Prediction and Analysis of Medium-to-Long-Range Boundary Reverb*, NRL Report 8721, NRL, Washington, DC, May 1984.

Ingenito, F., "Scattering from an object in a stratified medium", *J. Acoust. Soc. Am.*, 80, pp. 2051-2059, December 1987.

Ingenito, F. and S. N. Wolf, "Site dependence of wind-dominated ambient noise in shallow water", *J. Acoust. Soc. Am.*, 85(1), pp. 141-145, January 1989.

Jones, M. R., J. P. Riley, and T. M. Georges, *HARPO: A Versatile Three-Dimensional Hamiltonian Ray-Tracing Program for Acoustic Waves in an Ocean with Irregular Bottom*, Wave Propagation Laboratory, Boulder, CO, October 1986.

Kinsler, L. E., A. R. Frey, A. B. Coppens, and J. V. Sanders, *Fundamentals Of Acoustics*, John Wiley & Sons, New York, 1982.

Ly, L. N. and C. -S. Chiu, "*Coastal Acoustic Tomography Data Constraints Applied to a Coastal Ocean Circulation Model*", Technical Report, Naval Postgraduate School, Monterey, (1994).

Mykyta, J. L., Prediction of the Plane Wave Beamformed Acoustic Arrival Structure for the 1992 Barents Sea Coastal Tomography Test, Master's Thesis, Naval Postgraduate School, Monterey, 1993.

Newhall, A. E., J. F. Lynch, C.-S. Chiu, and J. R. Daugherty, "Improvements in the three-dimensional raytracing codes for underwater acoustics", *Computational Acoustics*, v. I., 1987.

Perkins, J. S., W. A. Kuperman, F. Ingenito, and L. T. Fialkowski, "Modeling ambient noise in three-dimensional ocean environments", *J. Acoust. Soc. Am.*, 93(2), pp. 739-752, February 1993.

Pierce, Allan D. and R. N. Thurston, eds., *High Frequency and Pulse Scattering: Physical Acoustics Vol. XXI*, Academic Press, Inc., Boston, 1992.

Pierce, A. D. and R. N. Thurston, eds., *Underwater Scattering and Radiation: Physical Acoustics Vol. XXII*, Academic Press, Inc., Boston, 1993.

Svardstrom, Anders, "Neural network feature vectors for sonar targets classifications", *J. Acoust. Soc. Am.*, 93(5), pp. 2656-2665, May 1993.

Urick, R. J., *Principles of Underwater Sound*, McGraw-Hill, Inc., New York, 1983.

Wenz, G. M., "Acoustic Ambient Noise in the Ocean: Spectra and Sources", *J. Acoust. Soc. Am.*, 34(12), pp. 1936-1956, December 1962.

INITIAL DISTRIBUTION LIST

		No. Copies
1.	Defense Technical Information Center Cameron Station Alexandria, Virginia 22304-6145	2
2.	Library, Code 52 Naval Postrgaduate School Monterey, California 93943-5101	2
3.	Director, Submarine Warfare Division Chief of Naval Operations (N87) Pentagon Room 4E453 Navy Department Washington, DC 20350-2000	1
4.	Director, Expeditionary Warfare Division Chief of Naval Operations (N85) Pentagon Room 4A720 Navy Department Washington, DC 20350-2000	1
5.	Professor Ching-Sang Chiu Code OC/Ci Naval Postgraduate School 833 Dyer Road Monterey, California 93943-5114	1
6.	Professor James H. Miller Code EC/Mr Naval Postgraduate School 833 Dyer Road Monterey, California 93943-5114	4
7.	Warren G. Huelsnitz 6320 7th Street NE Fridley, Minnesota 55432	1

8. Professor Robert M. Keolian — 1
Code PH/Kn
Naval Postgraduate School
833 Dyer Road
Monterey, California 93943-5114

9. Professor Harold A. Titus — 1
Code EC/Ts
Naval Postgraduate School
833 Dyer Road
Monterey, California 93943-5114

10. Oceanography Department — 1
Code OC/Bf
Naval Postgraduate School
833 Dyer Road
Monterey, California 93943-5114

11. Physics Department — 1
Code PH/Cw
Naval Postgraduate School
833 Dyer Road
Monterey, California 93943-5114

12. Naval Research Laboratory — 1
8555 Overlook Ave SW
Washington, DC 20375-5350
Attn.: Dr. Charles F. Gaumond, Code 7132

13. Naval Research Laboratory — 1
8555 Overlook Ave SW
Washington, DC 20375-5350
Attn.: Dr. L. Bruce Palmer, Code 7140

14. Chief of Naval Research — 1
Office of Naval Research
800 North Quincy St.
Arlington, VA 22217-5660
Attn: Mr. Tommy Goldsberry